Eur Biophys J (1999) 28: 317–329

ARTICLE

W. Wallinga · S.L. Meijer · M.J. Alberink · M. Vliek
E.D. Wienk · D.L. Ypey

Modelling action potentials and membrane currents of mammalian skeletal muscle fibres in coherence with potassium concentration changes in the T-tubular system

Received: 5 May 1998 / Revised version: 27 October 1998 / Accepted: 19 January 1999

Abstract During prolonged activity the action potentials of skeletal muscle fibres change their shape. A model study was made as to whether potassium accumulation and removal in the tubular space is important with respect to those variations. Classical Hodgkin-Huxley type sodium and (potassium) delayed rectifier currents were used to determine the sarcolemmal and tubular action potentials. The resting membrane potential was described with a chloride conductance, a potassium conductance (inward rather than outward rectifier) and a sodium conductance (minor influence) in both sarcolemmal and tubular membranes. The two potassium conductances, the Na-K pump and the potassium diffusion between tubular compartments and to the external medium contributed to the settlement of the potassium concentration in the tubular space. This space was divided into 20 coupled concentric compartments. In the longitudinal direction the fibre was a cable series of 56 short segments. All the results are concerned with one of the middle segments. During action potentials, potassium accumulates in the tubular space by outward current through both the delayed and inward rectifier potassium conductances. In between the action potentials the potassium concentration decreases in all compartments owing to potassium removal processes. In the outer tubular compartment the diffusion-driven potassium export to the bathing solution is the main process. In the inner tubular compartment, potassium removal is mainly effected by re-uptake into the sarcoplasm by means of the inward rectifier and the Na-K pump. This inward transport of potassium strongly reduces the positive shift of the tubular resting membrane potential and the consequent decrease of the action potential amplitude caused by inactivation of the sodium channels. Therefore, both potassium removal processes maintain excitability of the tubular membrane in the centre of the fibre, promote excitation-contraction coupling and contribute to the prevention of fatigue.

Key words Action potential model · Inward rectifier · Sodium-potassium pump · Tubular potassium concentration · Muscle fatigue

W. Wallinga (✉) · S.L. Meijer · M.J. Alberink · M. Vliek
E.D. Wienk
Department of Signals & Systems, BME,
Faculty of Electrical Engineering, University of Twente,
P.O. Box 217, 7500 AE Enschede, The Netherlands,
e-mail: w.wallinga-dejonge@el.utwente.nl

D.L. Ypey
Leiden University Medical Centre, Department of Physiology,
Leiden, The Netherlands

Introduction

It is quite common to simulate action potentials of skeletal muscle fibre membranes with the most prominent membrane properties. Sometimes the processes controlling the resting membrane potential are summarised as a leak current (Cannon et al. 1993; Henneberg and Roberge 1997). Because we wanted to model all currents per ion type we inserted the sodium, potassium and chloride conductances as experimentally determined and described in the literature. Since the chloride conductance represents 80% of the resting membrane conductance (Bretag 1987) it may serve to buffer membrane potential changes arising from changes in other conductive pathways. A particular phenomenon in skeletal muscle fibre activity is the accumulation of potassium in the tubular system. During each action potential the potassium concentration rises by 0.4 mM (Barchi 1994; Kirsch et al. 1977). If no removal of the potassium is achieved before succeeding action potentials, this will depolarise the membrane of especially the T-tubules. We have explored the ionic mechanisms of tubular potassium accumulation and removal processes by using a computer model to calculate the changes in the potassium concentration in the tubular system. The propagated action potentials and currents along the tubular and surface membranes were simultaneously simulated. We also investigated whether an increased tubular potassium concentration could cause an inward potassium current through the channels of the inward rectifier and by the Na-K pump in the tubular membranes. This inward current might counteract the accumulation of

potassium and prevent loss of excitability of the muscle fibre membranes during repeated firing.

If the potassium concentration in the tubular system is one of the desired outputs of the model, the description of the resting membrane potential has to include the essential potassium currents. Besides the classical Hodgkin-Huxley type sodium and potassium (delayed rectifier) currents, the present model includes a chloride, an inward rectifier, a Na-K pump and diffusion currents. When possible, the process descriptions and parameter values in the model are derived from measured mammalian muscle fibre properties. The incorporated chloride conductance represents the ClC-1 channels of mammalian muscle fibres (Pusch et al. 1994). The inward rectifier representation had to be based on data obtained from frogs (Standen and Stanfield 1978). In the Na-K pump description, voltage and intracellular sodium concentration dependency is combined with an extracellular sodium concentration-dependent factor (Nakao and Gadsby 1989; Luo and Rudy 1994; Siegenbeek van Heukelom 1994).

In skeletal muscle fibres the extensive tubular network and the properties of the tubular membrane do influence the propagated action potential, as already shown in 1973 by Adrian and Peachey. The model of the present study incorporates the currents indicated above in a cable model of the T-system with 20 compartments (as in Henneberg and Roberge 1997) and in the 56 segments of the sarcolemmal cable along the longitudinal axis of the fibre.

The aim of this study is to analyse tubular potassium accumulation and its effects on action potentials, during a 1-s period of firing at a physiological frequency. The inward rectifier appeared to be very important for the establishment of a new steady-state potassium concentration in the compartments of the tubular system during a train of 40 action potentials during 1 s. The inward rectifier channels essentially contributed to the maintenance of excitability. When the inward current through them was eliminated in the model, potassium accumulation was considerably enhanced. In this *manipulated* condition the action potentials were strongly reduced in amplitude and prolonged in time.

Another current effectively removing potassium from the tubular space is the current through the Na-K pumps. However, in the present paper the description of this and its parameters have not been varied. The reliability of the model components and results are discussed. Possible implications for the mechanism of muscle fatigue are briefly indicated.

Theory

The model

General

A multi-compartmentalised T-system model (abbreviated MCTS) has been used for the simulations. The muscle cell is represented as an intracellular space, suspended in a good conducting medium and in between them is the sarcolemma, according to Adrian and Peachey (1973). The model is composed of several longitudinal segments with transverse compartments representing the tubular system. The segments and compartments are described first and then the membrane conductances will be considered. The model choices (structural and parametrical) are, preferably, for mouse fast skeletal muscle fibres at room temperature. When other data had to be used this is indicated. The nomenclature is given in the glossary in Appendix 1. All equations are listed in Appendix 2 and Table A 2-1. The parametrical information is listed in the three tables of Appendix 3 (Tables A 3-1 – A 3-3). The change in the tubular potassium concentration is the most prominent ionic concentration change in and around muscle fibres (see discussion). It is the only concentration that is calculated in the model (last equation in Appendix 2).

The longitudinal segment and its transverse compartmentalisation

The tubular system is considered as a radial cable representing the volume average of the tubular system within a longitudinal segment of an axisymmetrical fibre (e.g. Adrian and Peachey 1973). The tubular system is divided into a number of concentric compartments, which form the elements of the radial cable (Fig. 1). Each tubular compartment has one uniform potential. All intracellular compartments within a longitudinal segment have the same potential, which differs from the tubular compartmental potentials.

The tubular and intracellular compartments are connected to each other as illustrated in Fig. 2. The extracellular space and the tubular system are coupled by a resistive interface layer (with resistance R_a, see Fig. 2) at the mouth of the tubules (at the external rim of the outer compartment). The tubular current I_T flows through R_a. The

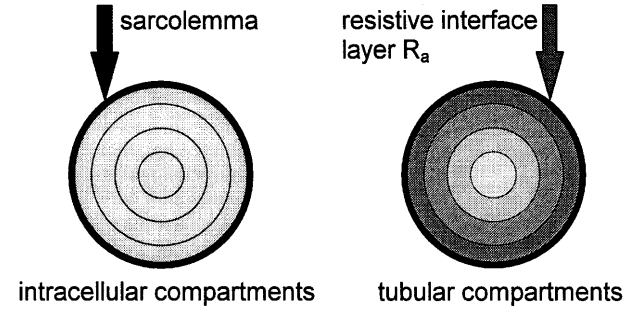

Fig. 1 Cross-section of a fibre segment divided into concentric compartments. In the *left part* the cross-section displays the intracellular compartments, which are all similar except for their volume. The tubular compartments are depicted in the *right part.* Here a compartment represents a volume, each with its own homogeneous amount of T-system (0.3 vol%) and its own potassium concentration. In the model a tubular compartment interacts with the corresponding intracellular compartment. These two compartments are separated by the tubular membrane

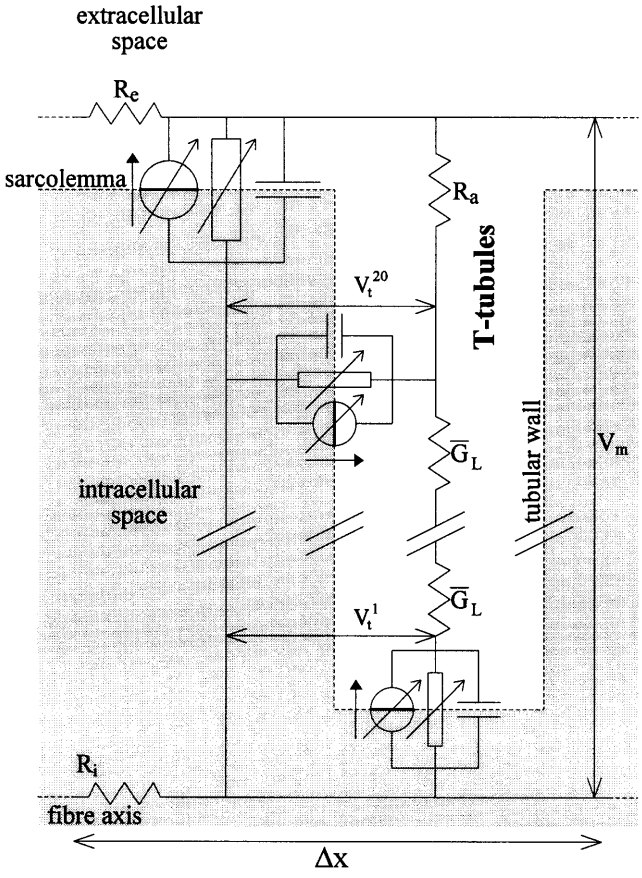

Fig. 2 Longitudinal segment of a fibre, including the voltage-dependent Na-K pump (denoted by a voltage-dependent current source), the voltage-dependent non-linear conductivity of the passive ion currents (represented as voltage-dependent impedances) and the membrane capacity. The T-system is represented as a radial cable from the fibre surface to the fibre axis. Each cable element represents a volume averaged part of the T-system, with a tubular membrane potential V_t^i and a tubular cable conductivity, G_L. The tubular current I_T flows through the access resistance R_a out of the tubules into the extracellular space. R_e and R_i are the extracellular and intracellular resistivities, respectively. The intracellular potential is V_m, which is the potential across the sarcolemma. The tubular potential, V_t^i, is the potential across the tubular membrane in compartment *i*

electrical circuit representation of a longitudinal segment of the muscle fibre is given in Fig. 2. Here the circuit of Henneberg and Roberge (1997) is extended with the Na-K pump and the voltage-dependent conductances include more species (see section Description of membrane conductances).

Concatenation of the longitudinal segments

Our model consists of a concatenation of longitudinal fibre segments of length Δx, according to Adrian and Marshall (1976). Figure 3 presents a scheme of the MCTS model.

Descriptions of the membrane conductances

The total surface membrane current includes a capacitive current, a tubular current and a summation of several ionic currents. The total ionic current is composed of the sodium current (activation, fast inactivation and slow inactivation), the delayed rectifier potassium current (activation, slow inactivation), the inward rectifier potassium current, the chloride current and the Na-K pump current. New elements with respect to Cannon et al. (1993) are the slow sodium and potassium inactivation processes, the replacement of the leak current by a combination of the inward rectifier and the chloride and the addition of Na-K pump currents. The new parts of our MCTS model are now described.

Slow inactivation of sodium conductance. Slow inactivation cannot be neglected at the resting membrane potential (Ruff et al. 1988; rat muscle). Therefore, these experimental data are used to describe slow sodium inactivation. Their description is adapted for the ionic composition of the spaces in the MCTS model.

Slow inactivation of delayed rectifier conductance. When the membrane potential remains at values less negative than the normal resting membrane potential for more than

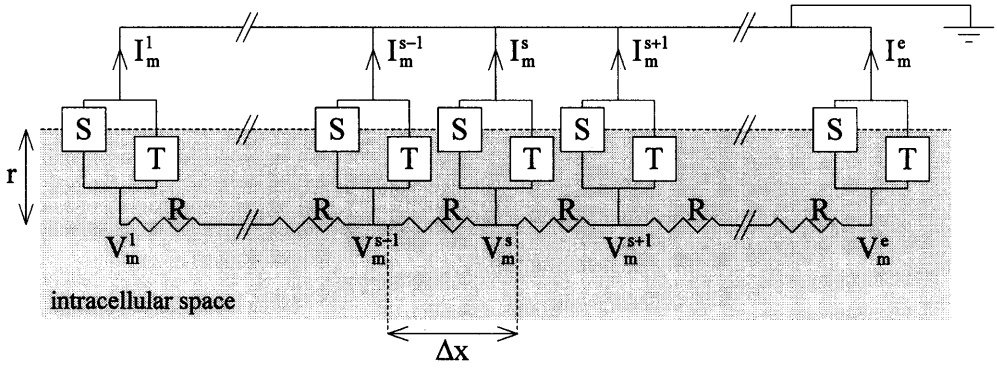

Fig. 3 Longitudinal segmented representation of the muscle fibre in the complete MCTS-model. I_m^s is the total surface membrane current (sarcolemmal plus tubular current) in segment *s*. V_m^s is the potential of the intracellular space at segment *s*, which is the potential difference across the sarcolemma. S and T denote the non-linear properties of the sarcolemma and of the radial cable representing the T-system, respectively. The fibre radius is denoted by *r* and *R* is the resistance between two adjacent segments, given by $\Delta x\, R_i/\pi\, r^2$ [Ω]

100 ms, there is an apparent effect on the current-voltage relation of the delayed rectifier. Therefore, slow inactivation of this potassium conductance is inserted into the MCTS model with a Boltzmann distribution function and a time constant (τ_{h_K}) according to Adrian et al. 1970 (data obtained from frogs).

Inward rectifier conductance. The inward rectifier conductance is important for the behaviour of the MCTS model, which primarily applies to mouse muscle. However, because of lack of mammalian data the inward rectifier description had to be based upon data obtained from frogs (Standen and Stanfield 1978). There is a strong effect of potassium concentration on the inward rectifier current. The varying potassium concentration in the tubular compartments results in different inward rectifier currents in the 20 compartments of the tubules. The MCTS model does not include inactivation for the inward rectifier. There is hardly any inactivation around the resting membrane potential (Matsuda and Stanfield 1989). The densities of the inward rectifier channels in the sarcolemmal and tubular membranes in frog muscles are equal (Ashcroft et al. 1985). This is assumed in our model as well. Hence, the ratio of the densities of these channels in the tubular and surface membranes is 1 (η_{IR} is 1).

Chloride conductance. The instantaneous relation between current and voltage of ClC-1 channels (Pusch et al. 1994) is used to define chloride conductance. Their instantaneous and steady state *I-V* relationships nearly coincide in the relevant potential range. Therefore the simpler instantaneous relation was used in our model. In the MCTS model the curve is shifted to match the resting membrane potential of the model and the fit is realised with a Boltzmann distribution function "*a*" (see equation of chloride conductance in Appendix 2 and for its parameter "*a*" in Table A 2-1). The current-voltage relation in our model is similar to the experimental instantaneous one described by Fahlke and Rüdel (1995). The chloride channels constitute 80% of the total sarcolemmal membrane conductance at rest (Bretag 1987), which is set at about 2.4 mS/cm^2 in our model (as in Cannon et al. 1993). Consequently the chloride conductance is 1.9 mS/cm^2 at rest, which resulted in a maximum chloride conductance of 6.55 mS/cm^2. Despite the fact that Gurnett et al. (1995) only showed ClC-1 channels in the sarcolemma, the density of the chloride channels in the tubular membrane was chosen 0.1 times the sarcolemmal density. In fact we account in this simplified way for the presence of other chloride channels in the tubular membrane (Dulhunty 1979).

Na-K pump. The Na-K pump description comprises a voltage-independent part according to Siegenbeek van Heukelom (1994) and a voltage-dependent part according to Nakao and Gadsby (1989) in the same way as used by Luo and Rudy (1994). The kinetic constants of the Na-K pump have been chosen such that the influence on the resting membrane potential is small, preventing the chloride current from being persistently large at rest. Elimination of the Na-K pump shifted the membrane potential by 0.6 mV. This is low in the range of literature values (less than 1 mV in Seabrooke et al. 1988; a few mV in Hicks and McComas 1988; 10 mV in Läuger 1991). The density of Na-K pumps is lower in the tubular membranes than at the fibre surface (Fambrough et al. 1987). In the model the difference is a factor 0.1.

Model parameters

The background of some important parameter choices is presented here.

Our *tortuosity factor*, σ_T, is a little higher than the value of Mathias et al. (1977) in relation to the longer sarcomere length of mouse EDL fibres than that of frog fibres.

The *conductivity of the lumen*, G_L, in the tubular system has an important effect on the average tubular conduction velocity, θ_T, defined as the fibre radius divided by the time delay between the peaks of the action potentials at the sarcolemma and at the fibre axis. We have assumed an average tubular conduction velocity of about 2.5 cm/s for the muscle fibres with a diameter of 40 μm (diameter as in Luff and Atwood 1972). In the MCTS model this criterion is met by taking the lumen conductivity as 3.7 mS/cm.

The *average tubular potassium accumulation* per action potential is about 0.4 mM (Barchi 1994; Kirsch et al. 1977). This accumulation is fitted by the choice of the ratios η (see Appendix 1 and Table A 3-2) of the delayed and inward rectifier channel densities between the tubular and surface membranes. As indicated previously, the value used for η_{IR} is 1, making the density of inward rectifying channels in the tubular membrane the same as that in the sarcolemma (according to Ashcroft et al. 1985). In the MCTS model the average tubular potassium accumulation is 0.4 mM when $\eta_{DR} = 0.45$. This value is used for the ratio of the delayed rectifier channel density. It is close to the value of 0.4 used by Cannon et al. (1993).

Methods

Model environment

The equations form one set of differential equations which is implemented in programming language C. Solving this set over a simulation time of 250 ms, using a fourth- and fifth-order Runge-Kutta-Fehlberg method with variable step size on a HP series 700/RX, takes about 12 h for 56 longitudinal segments each with 20 tubular compartments. The choice of the numbers 56 and 20 is explained in the first section of the results. The end condition at 250 ms represents the starting condition for the next 250 ms, up to 1 s in total. No parameter of the MCTS model in the reference set has a critical value, but small changes in the values of some parameters may still change the behaviour of the model. Owing to long simulation times, parameter variation is tested mainly in simulations with the model comprising one segment.

Model responses

In the preceding sections the information concerned the reference model, including the reference set of parameters (standard model properties). The responses of the reference model suggested an important role of the inward rectifier in the removal of potassium from the tubules. In order to demonstrate the effects of increased potassium levels in the tubules adapted, it was chosen to set $I^{i}_{\mathrm{IR},t}$ in the last equation of Appendix 2 to zero, when its value was negative. Consequently, only the removal of potassium by the inward rectifier is not possible. In this so-called *manipulated* model everything is normal except the potassium transient in the tubular space. Results will be presented for the reference and *manipulated* conditions.

Summarising, the reference simulation results had to meet the following six requirements:

1. A stable and normal resting membrane potential (Luff and Atwood 1972).
2. 80% of the resting membrane conductance is carried by the chloride conductance.
3. The potassium accumulation equals about 0.4 mM per action potential.
4. The values of the conduction velocity along the sarcolemma (own unpublished results on mouse EDL muscle at room temperature) and the tubular membrane (Nakajima and Gilai 1980) are physiologically correct.
5. The shape of the propagated action potential is natural (own unpublished results on mouse EDL muscle at room temperature).
6. The shape of the total membrane current is similar to recorded ones (Wolters et al. 1994).

The reference process descriptions and parameter values are consistent with these prerequisites (see first section of results).

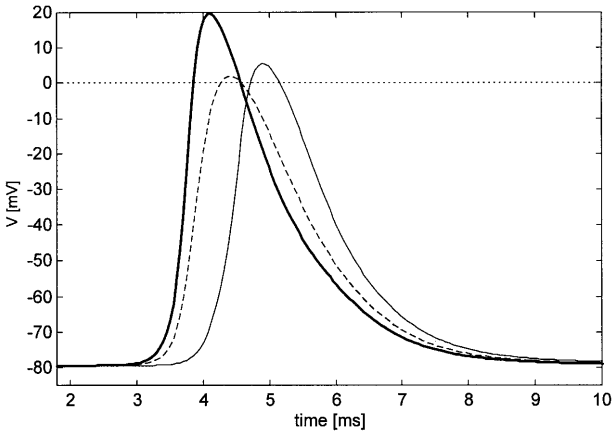

Fig. 4 The first action potential in a train of 40 action potentials at the sarcolemma (*bold*), the tubular membranes of the inner compartment of the T-system (*normal*) and the tubular membranes of the outer compartment of the T-system (*dashed*)

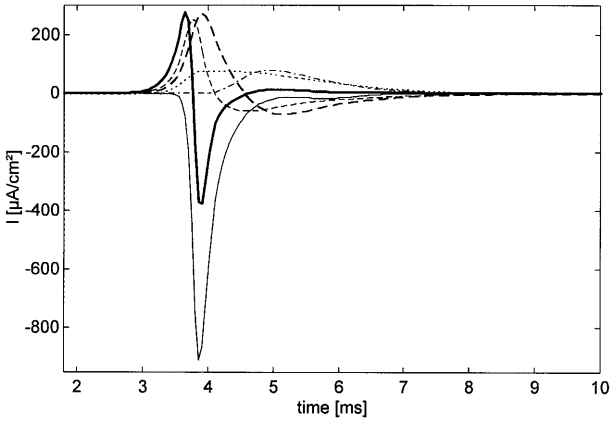

Fig. 5 Surface membrane current densities during the first action potential of a train: total (*bold*), sodium (*normal*), capacitive (*dashed*), chloride (*dotted*), delayed rectifier potassium (*normal dashed-dotted*), tubular current, I_{T} (*bold dashed*). The inward rectifier is not plotted here because it is relatively small

Results

MCTS model check

First, condition and parameter choices of the reference model are illustrated with simulation results. Stimulation with current pulses was identical in all simulations and was applied in the first segment (the farthest away from the middle segment) by clamping the membrane to a current density of 80 µA/cm^2 for 0.85 ms. This stimulus pulse evoked action potentials that became stable rather quickly during propagation away from the stimulus site. The stimulation interval was within the natural range of intervals (20–200 ms) (De Luca and Erim 1994). The chosen 25 ms interval was rather short for enhancing the effects of multiple stimulation. All results were simulated with the length of all longitudinal segments set at 100 µm. Smaller lengths hardly changed (change < 0.5%) the waveform and the conduction velocity of the propagated action potentials. The electrical behaviour of the fibre membrane near the sealed ends showed ending effects, i.e. the action potentials approaching the fibre ends had an increased longitudinal conduction velocity and peak sarcolemmal potential compared to action potentials in the middle segments (according to the results of Adrian and Marshall 1976). Test simulations showed that, with 56 longitudinal segments, the segments around the 30th had a constant action potential and conduction velocity. Therefore, this 30th segment was used for the results presented in this paper.

In comparison with all other compartments, the behaviour of the outer tubular compartment depends, above all, on the presence of the access resistance. In our model the number of 20 tubular compartments was equal to that in Henneberg and Roberge (1997). Here, the sarcolemmal action potential and the average tubular conduction velocity are insensitive to the number of compartments.

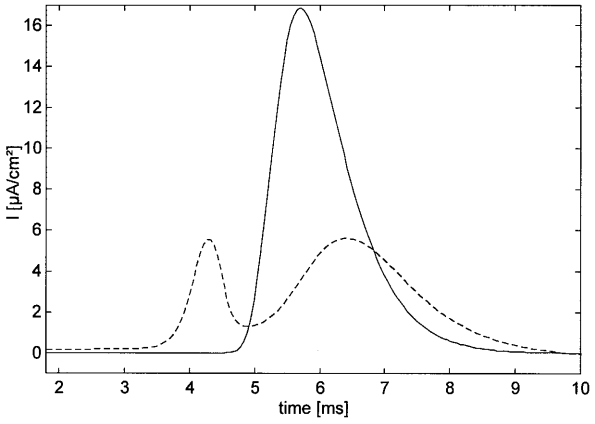

Fig. 6 Current density of delayed (*line*) and inward rectifier (*dashed*) in the tubular membrane of the inner compartment during the first action potential of a train

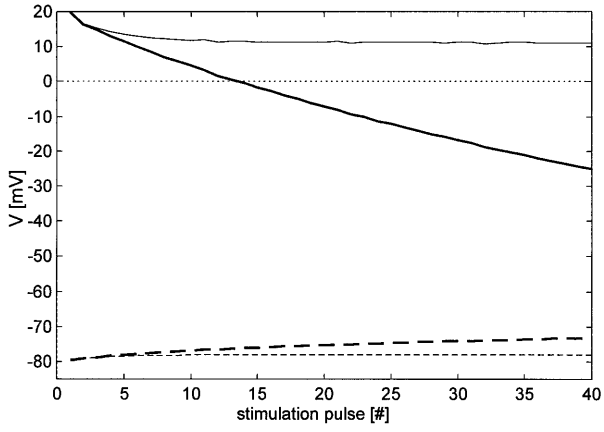

Fig. 7 Tops of action potentials (*solid*) and resting membrane potentials (*dashed*) in a train of sarcolemmal action potentials with 25 ms interval times in two situations. The reference is plotted normally and the situation when cancelling the inward current of potassium through the inward rectifiers (*manipulated*) boldly. Resting membrane potentials are measured just before each stimulation

In Fig. 4 the sarcolemmal and tubular action potentials following the first stimulation pulse of a train are plotted. The results meet the requirements listed above. The resting membrane potential equalled −80 mV. The mean potassium concentration in the tubular space increased by 0.4 mM at the first action potential. The conduction velocity along the sarcolemma was 1.6 m/s, while the average tubular conduction velocity was 2.5 cm/s. The tubular conduction velocity was lower than 6.4 cm/s, which is the value for frog measurements by Nakajima and Gilai (1980). The smaller diameter of mammalian T-tubules should cause a lower velocity. The shape asymmetry of the propagated action potential (a shorter rising than declining phase) was similar to recorded action potentials. The shape of the membrane current (Fig. 5) was good, but the relative amplitude of the third phase was rather small in the simulation.

Model behaviour when starting an action potential train

The shape of the tubular action potentials (Fig. 4) depended on the radial location as in Adrian and Peachey (1973). The various ionic currents of the sarcolemma behaved during the action potential as shown in Fig. 5. The inward sodium current was the largest. The outward capacitive current from the sarcolemmal membrane and the tubular current already started before the sodium current. These three currents were the main components up to the negative peak of the total current. The outward chloride current followed the action potential instantaneously, while the outward delayed rectifier current showed a significant delay. The tubular current through the access resistance was caused by a potential difference between the tubular lumen and the extracellular medium. The tubular current was dominated by the capacitive component of the tubular membrane, so consequently the shapes of the capacitive sarcolemmal current and the tubular current were rather similar. During the third phase of the current pattern, the outward chloride and delayed rectifier potassium currents were comparable in size with the inward sarcolemmal capacitive and tubular currents. As a result the third phase is small.

The increase in the tubular potassium concentration during an action potential occurred by means of the outward potassium current through both the delayed rectifier and inward rectifier conductances. In the first action potential their contributions were about equal (Fig. 6). In the plotted time span there was no transport back to the sarcoplasm, since the potassium currents were outward during the action potential. Between 10 and 25 ms (when the next stimulus was on its way) the inward rectifier conducted a very slight amount of potassium into the sarcoplasm from the tubular compartments. The accumulated tubular potassium (rise by 0.4 mM to a maximum of 6.8 mM) brought the potassium equilibrium potential just above the membrane potential. This inwardly directed potassium component was always absent for the sarcolemma, because the potassium concentration in the surrounding space was fixed at one value (5.9 mM).

Model behaviour during an action potential train

After the reference parameter values of the model were chosen in single-pulse stimulation, simulations were run for stimulus trains. Owing to tubular potassium accumulation the resting membrane potential shifted less than 2 mV towards zero and the tops of the sarcolemmal action potentials dropped by 9 mV, as shown in Fig. 7. At the same time the action potentials became broader (details are presented in the text related to Fig. 10). After 15 stimuli there was no further change in the responses.

The changes in the action potentials of the membranes in the centre compartment were a little larger than those of the sarcolemma. Centrally there was a continuous change in resting membrane potential from −79 to −77 mV and the peak value of the action potential shifted from +5 mV at the first action potential to −5 mV in the 40th. In the case

of the central tubular membranes the potassium equilibrium potential shifted during the train of action potentials from −80 to −74 mV, while its value for the sarcolemma stayed at −82 mV. Owing to the influence of the chloride conductance the tubular membrane potential reached a value more negative than the new potassium equilibrium potential value. Consequently, this tubular membrane potential enabled the inward rectifier channels to conduct a noticeable inward current and to remove potassium from the tubular space (see results presented below). Note that although the tubular resting membrane potential is less strongly set by chloride ions than the sarcolemmal one (because the chloride channel density is 0.1 times the sarcolemmal density), this membrane potential was still negative enough to drive inward current through the inward rectifier conductance (results presented in Fig. 8).

For the *manipulated* case (with cancelled potassium reuptake from the tubular space by means of the inward rectifier channels as described in the section on Theory) the changes in the resting membrane potential and action potentials during the stimulation series (bold curves in Fig. 7) were enhanced with respect to the reference case (normal curves). The differences between the lines clearly show that the artificially increased potassium concentration in the tubular compartments shifted the resting membrane potential gradually during the whole stimulation period to 6 mV lower negative values and, consequently, reduced the amplitudes of the sarcolemmal action potentials by increased sodium inactivation from 100 to 49 mV (cf. Figs. 4 and 10).

Not shown in a figure are the changes in the central compartment of the T-tubules. The resting membrane potential shifted from −79 to −68 mV and the action potential amplitude from 83 to 30 mV. Here the shift of the potassium equilibrium potential from −79 to −62 mV strongly enhanced the inward potassium flow through the inward rectifier.

In Fig. 8 the potassium concentration is followed in time during the 1 s stimulation period, again for the reference (normal curves) and *manipulated* (bold curves) model, in both the centre and in the outer compartment of the tubules. The reference contributions of the various currents involved in the potassium concentration changes of the centre compartment are displayed in Fig. 8a. The curves represent the contributions of four potassium currents to the tubular concentration in the centre compartment during the train of 40 action potentials. These contributions sum up to the curve labelled “total”. The diffusion component is the potassium current carried by diffusion to and from the neighbouring compartments. While the diffusion component was about zero in the centre compartment, its size was the largest one in the outer compartment owing to the apparent concentration difference between the outer compartment and the external medium at its fixed concentration of 5.9 mM (results not shown). Figure 8a clearly shows that the delayed rectifier continued to be responsible for potassium accumulation in the centre compartment (see curve DR), while the inward rectifier (IR) was consistently an important conductor in both directions be-

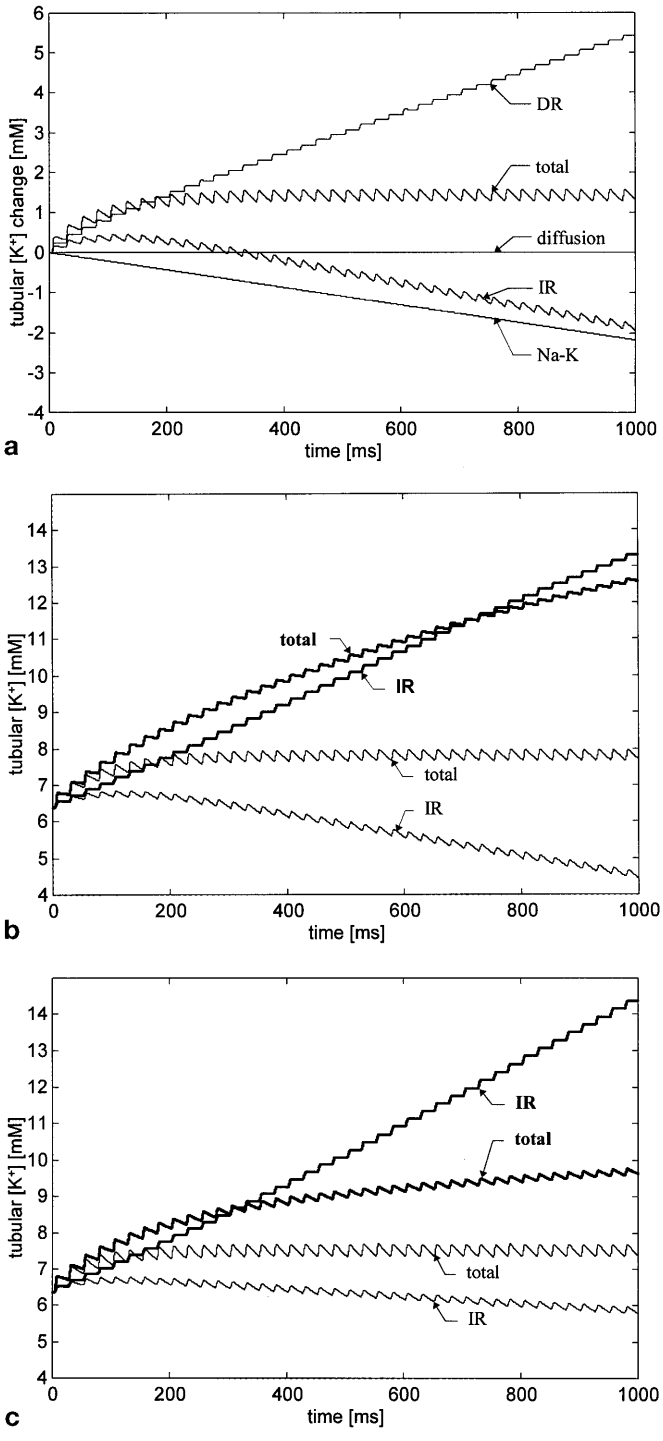

Fig. 8a The contributions of the discerned potassium currents to the potassium change in the centre tubular compartment are plotted for the normal situation. The contribution of the inward rectifier is labelled IR, that of the delayed rectifier DR, that of the Na-K pump Na-K and the diffusion label is given to the summed component of the diffusion current to and from neighbouring compartments. The curve “total” represents the sum of all contributing currents. **b** Potassium concentrations in the centre tubular compartment during the train of action potentials. Labelling is according to **a**. Total and IR curves are given for the reference (*normal*) and *manipulated* (*bold*) situation. **c** Identical to **b** for the outer tubular compartment

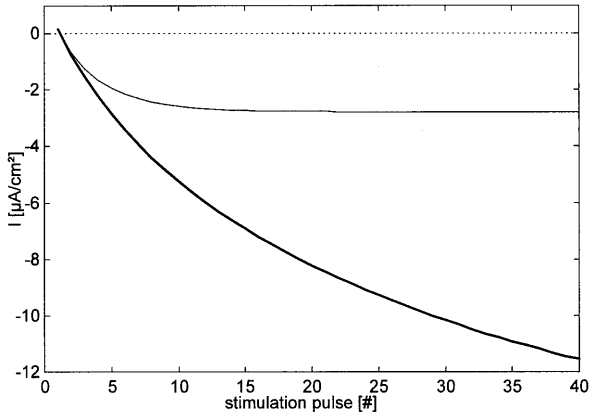

Fig. 9 Current densities from T-tubules (I_T) through access resistance R_a just before each stimulation pulse begins versus the stimulation pulse number, in reference (*normal*) and *manipulated* (*bold*) situation. A negative current density represents an inward tubular current density

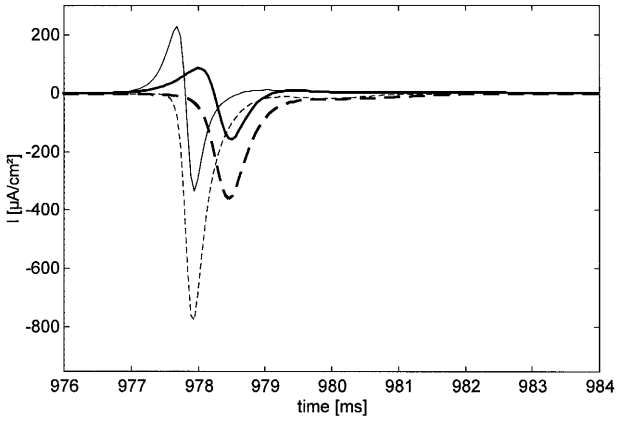

Fig. 11 Total (*solid*) and sodium (*dashed*) current densities of the sarcolemma during the final action potential of the train in the reference (*normal*) and *manipulated* (*bold*) situation

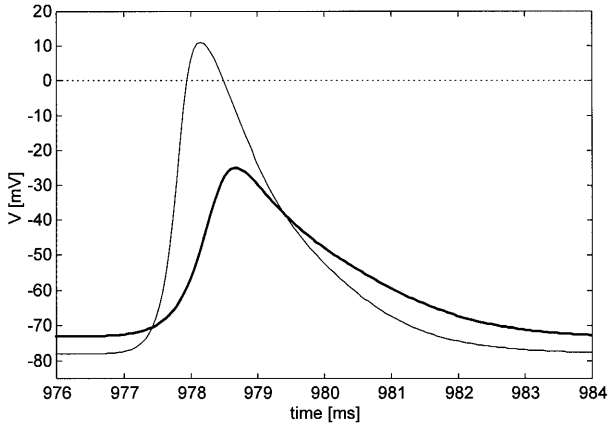

Fig. 10 Final sarcolemmal action potentials of the train in the reference (*normal*) and *manipulated* (*bold*) situation

tween the sarcoplasm and the tubular space. Up to the fifth action potential, accumulation surpassed clearance per action potential. After the sixth action potential, IR clearance caused a decrease of the tubular potassium concentration.

Note also how strongly the Na-K pump removed potassium during the train. This occurred with a density of Na-K pumps introducing only 0.6 mV effect in the resting membrane potential. Moreover, the ratio of the tubular to sarcolemmal pump densities was small (0.1).

Figure 8b (centre compartment) and c (outer one) focus on the *manipulated* model, resulting in a comparison with those of the reference model for the inward rectifier and total curves. In the starting condition the potassium concentration in both compartments was about 0.5 mM above the concentration around the fibre. In the normal case the potassium concentration increased up to about 300 ms. After this the ripple became constant. The mean final level of the two compartments differed, being 0.3 mM higher at the centre. In the *manipulated* case the increase in potassium concentration caused by all contributing potassium currents together took more time to level off and was about 3 mM higher at the centre than at the outer compartment during the end of the action potential train. The Fig. 8b and c plots confirm the conclusion that the inward potassium flow through the inward rectifier was apparent in all compartments. In the centre compartment in the normal model it significantly contributed to the prevention of potassium accumulation.

The access resistance at the rim of the outer tubular compartment and the strong potassium gradient at that location influenced the processes going on locally. Since the physical correctness of these two aspects is open for question, the results of the outer compartment are not presented in as much detail as those of the inner one.

In Fig. 9 the lines in the plot show that the tubular circuit current (I_T) due to the developing difference in the sarcolemmal and outer compartmental tubular membrane potential was strongly enlarged in the *manipulated* simulation. The accompanying tubular circuit current went inwardly into the tubules. The positive resulting shift in the resting membrane potential of the sarcolemma during the action potential train has already been shown in Fig. 7.

In the next two figures the sarcolemmal behaviour is given for the final evoked action potential at the end of the stimulation during 1 s. The amplitude of the reference sarcolemmal action potential was reduced by 10 mV and the shape became 15% broader (at one third of the action potential amplitude) for the final compared to the first action potential. In the case of the *manipulated* final action potential the broadening was by 50%. Then the action potential amplitude decreased by 51 mV (Fig. 10 versus Fig. 4).

In Fig. 7 it was already shown how dramatic the decrease of the action potentials in the centre compartment of the T-tubules was during the stimulation, especially in the case of the *manipulated* model. The dramatic reduction of the action potential amplitude (final amplitude only 30 mV) would seriously affect excitation-contraction coupling.

The changes in the total current and sodium component for the two conditions are shown in Fig. 11. Comparison of the membrane currents in Fig. 5 and 11 shows that under the reference condition the amplitude of the sarcolemmal membrane current density transients decreased by 15% during the series of 40 action potentials and the membrane currents became a little slower. The high level of potassium in the tubular space in the *manipulated* condition exaggerated strongly both phenomena.

Discussion

General

The present model provides a further integration of known electrophysiological properties for the quantitative study of excitation of the intact muscle fibre. Since the model includes many (56) successive fibre segments it offers the opportunity to study stationary propagated action potentials far removed from the stimulation site, taking into account the extensive tubular membrane system, during a prolonged period of time.

The introduction of chloride and inward rectifier currents and a Na-K pump encourages new applications. Here, principal attention is paid to the changes in membrane currents and action potentials in relation to potassium accumulation in the T-system. A model of extracellular potassium accumulation and removal for ventricular heart cells takes into account the delayed rectifier and an ATP-dependent current (Yasui et al. 1993). So far, the important role of the inward rectifier in the removal of potassium from the tubules in skeletal muscle fibres has received little attention (cf. van Mil 1997). Its function in the limitation of the slowing down in conduction of action potentials along nonmyelinated mammalian axons has recently been described by Grafe et al. (1997).

Complexity of the model: a compromise

Skeletal muscle performance depends heavily on the concentrations of sodium, potassium and chloride ions, on the extracellular fluid volume and pH (McKenna 1992) and on the calcium concentration (Fitts 1994). Here we focus on the tubular potassium concentration, which is by far the most important conditional parameter in the context of this paper. The change in the intracellular sodium concentration is small in comparison with the change in potassium concentration in the tubular system. The latter is a consequence of the potassium current into the small volume of the T-system through the large surface of its membrane (up to three times that of the sarcolemma; Luff and Atwood 1972). The inward rectifier only conducts inward current for tubular potassium clearing, if the resting membrane potential after firing is more negative than the potassium equilibrium potential. This condition is warranted by the effect of increased tubular potassium concentration on the potassium equilibrium potential and the high resting conductance to chloride ions that holds the membrane potential close to the chloride equilibrium potential.

In the model presented, the potassium current was carried by the delayed rectifier, the inward rectifier, the Na-K pump and the diffusion. We neglected the outflow of potassium by the ATP-sensitive potassium channels and the calcium activated potassium channels (McKenna 1992). These two types of potassium channels could also contribute to potassium accumulation in the tubular space during action potential firing, if they were to occur in the tubular membrane. In mammalian muscle fibres the ATP-dependent potassium channels are present in a high density in the sarcolemma, but they are not able to open, unless the pH is lowered (Davies 1992) or the ATP level is strongly reduced (McKillen et al. 1994). How the channels would affect the tubular potassium concentration after action potential firing remains as yet unclear. The Na-K pump properties in the model are certainly too simple. In vivo, its function is very sensitive to hormonal levels, contractile activity, growth and nutrition (Clausen 1996). Short- and long-term processes are mixed together and are not yet available for quantitative representation in a model. The Na-K pump parameters used in the model had a small density in the sarcolemma and a ten times smaller density in the tubular membrane. However, the Na-K pumps still removed slightly more potassium than the inward rectifier in the centre compartment of the tubules. The calculated tubular potassium concentration rise of 1.5 mM in the reference condition at the end of the stimulation is within the expected physiological range. Juel (1986) mentions a rise in extracellular potassium concentration up to 5 mM, Sjøgaard and McComas (1995) up to 15 mM, but still higher rises may occur in the tubular space.

The importance of the different potassium currents for the excitability of the membranes (sarcolemma and tubular membrane) is to be studied in more detail. Owing to the inaccessible localisation of the tubular membrane, experimental data will be very difficult to obtain, but for the time being modelling offers a tool to promote awareness of the possible roles of the various potassium currents.

Overall implications

The lack of interest in physiological functions of the inward rectifier is apparent in the literature, even when the role of interstitial potassium is considered (Sjøgaard and McComas 1995). The present paper emphasises that the inward rectifier could be important for the prevention of positive shifts of the resting membrane potential, especially in the tubular system of the skeletal muscle fibres. This role may also be important for the limitation of potassium accumulation in the small extracellular space around the muscle fibres (especially when blood circulation would be insufficient to refresh the extracellular medium). The inward rectifier is a suitable candidate for the prevention of fatigue in the scheme of Sjøgaard and McComas (1995).

Inward rectifier channels are potentially prominent controllers of the resting membrane potential, as shown in this paper. The behaviour of the inward rectifier depends on several intracellular signals (Wieland and Gong 1995). In our model, after activity the action potentials in the central tubular system reach an amplitude of only 30 mV, if the inward transport of potassium by the inward rectifier is hampered. This would seriously reduce the effectiveness of the excitation-contraction coupling processes. Therefore, the role of the inward rectifier in maintaining excitability and excitation-contraction coupling during repeated action potential firing remains an interesting subject for future research. In the centres of the tubules its role is almost as effective as the Na-K pump.

Appendix 1: Glossary

a	Boltzmann distribution function in formula of g_{Cl}
A_x	variables determining steepness of $x \in \{h_{K\infty}, S_\infty\}$ (mV)
A^s	surface of sarcolemma of one longitudinal fibre segment (cm^2)
A_t^i	amount of tubular membrane surface in compartment i (cm^2)
C_m	specific capacitance per unit area of surface and tubular membrane ($\mu F/cm^2$)
ClC-1	chloride channels
DR	delayed rectifying channels
E_{ion}	equilibrium potential of ion $\in \{Cl^-, K^+, Na^+\}$ (mV)
$f(V)$	voltage-dependent part of Na-K pump current density
F	Faraday's constant (C/mol)
g_{chan}	surface conductance of chan $\in$ {ClC-1, DR, IR, Na} (mS/cm^2)
$\hat{g}_{chan}$	surface maximum conductance of chan $\in$ {ClC-1, DR, IR, Na} (mS/cm^2)
$\hat{g}_{chan,t}$	tubular maximum conductance of chan $\in$ {ClC-1, DR, IR, Na} (mS/cm^2)
$g_{L,t}^i$	radial conductivity of one Δx fibre segment in compartment i (mS)
G_K	maximum conductance when all sites are filled with K^+ (mS/cm^2)
G_L	luminal conductivity of the T-tubulus (mS/cm)
$\bar{G}_L$	tubular cable conductivity (mS/cm)
h	variable of fast inactivation behaviour of sodium conductance
h_K	variable of inactivation behaviour of delayed rectifier conductance
$h_{K\infty}$	non-inactivated part of delayed rectifier channels in steady-state
$[ion]_i$, $[ion]_o$	intra- and extracellular concentration of ion $\in \{Cl^-, K^+, Na^+\}$ (mM)
I_C^s, I_C	surface capacitive component of I_m in segment s ($\mu A/cm^2$)
$I_{C,t}^i$	tubular capacitive component of $I_{m,t}^i$ in compartment i ($\mu A/cm^2$)
I_{chan}	surface current density through chan $\in$ {ClC-1, DR, IR, Na-K} ($\mu A/cm^2$)
$I_{chan,t}^i$	tubular current density in compartment i through chan $\in$ {ClC-1, DR, IR, Na-K} ($\mu A/cm^2$)
I_{ionic}^s, I_{ionic}	surface ionic component of I_m in segment s ($\mu A/cm^2$)
$I_{ionic,t}^i$	ionic component of $I_{m,t}^i$ in compartment i ($\mu A/cm^2$)
I_m^s, I_m	total surface membrane current density passing between sarcoplasm and extracellular fluid per unit area of surface membrane in segment s ($\mu A/cm^2$)
$I_{m,t}^i$	total tubular membrane current density passing between the sarcoplasm and the tubular lumen per unit area of tubular membrane in compartment i ($\mu A/cm^2$)
$\hat{I}_{NaK}$	voltage-independent part of Na-K pump current density ($\mu A/cm^2$)
I_T^s, I_T	total current density leaving tubular system per unit area of surface membrane in segment s ($\mu A/cm^2$)
IR	inwardly rectifying potassium channels
$\hat{J}_{NaK}$	maximum pump activity ($\mu mol/cm^2\ s$)
K_{mK}, K_{mNa}	affinity constants for $[K]_o$ and $[Na]_i$ (mM)
K_K, K_S	dissociation constants for K^+ ion and blocking cation S^+ (mM^2)
$[K]_R$	concentration of potassium at binding site (mM)
$[K^+]_t^i$	potassium concentration in compartment i of tubular system (mM)
l_f	length of simulated fibre (cm)
m	variable of activation behaviour of sodium conductance
MCTS	Multi-Compartmentalised T-System
n	variable of activation behaviour of delayed rectifier conductance
Na-K	sodium potassium pumps
r	fibre radius (cm)
r_i	radius of compartment i: (compartment number)$\times r/20$ (cm)
R	gas constant [J/(K mol)]
R_a	access resistance at entrance of the T-tubulus ($k\Omega\ cm^2$)
R_i, R_e	intra- and extracellular resistivity ($k\Omega\ cm^2$)
S	variable of slow inactivation behaviour of sodium conductance
$[S]_i$	intracellular blocking cation concentration (mM)
S_∞	variable of slow inactivation behaviour of g_{Na} in steady-state
t	time (ms)
T	temperature (K)
V^s, V	potential across the surface membrane in segment s, V general (mV)
V_x	voltage at which $x \in \{a, h_{K\infty}, S_\infty\}$ is at half its maximum value (mV)
V_t^i	potential difference across the tubular membrane in compartment i (mV)

Vol^i	volume of compartment i (cm^3)
Δx	length of one longitudinal fibre segment (cm)
y	fraction of inward rectifier channels that are open
α_x, β_x	rate constants in $x \in \{h, m, n\}$ (ms^{-1})
$\hat{\alpha}_x$	maximum rate constant in $x \in \{m, n\}$ (ms^{-1} mV^{-1})
$\hat{\alpha}_h$, $\hat{\beta}_x$	maximum rate constants in h and $x \in \{h, m, n\}$ (ms^{-1})
δ	fraction of electrical distance through membrane from outside, where binding site is placed
η_{chan}	ratio of channel density between tubular and surface membranes, chan ∈ {ClC-1, DR, IR, Na, Na-K}
ρ	fraction of muscle volume occupied by T-tubulus
σ	variable in voltage-sensitive part of $I_{Na\text{-}K}$, dependent on $[Na]_o$
σ_T	tortuosity factor: fraction of radial directed tubular branches
τ_{h_K}, τ_S	time constants in slow inactivation of DR and Na channels (s)
τ_K	time constant in passive first-order rate process of diffusion of potassium ions between adjacent tubular compartments (ms)
ζ	volume-to-surface-area ratio for T-tubules (cm)

Appendix 2: Model equations

$$I_m^s = \frac{(V^{s+1} - 2\,V^s + V^{s-1})\,\pi\,r^2}{\Delta x\,R_i\,A^s} = I_C^s + I_{ionic}^s + I_T^s$$

(^{s} is omitted in following equations)

$$A^s = 2\,\pi\,r\,\Delta x$$

$$I_C = C_m\,\frac{dV}{dt}$$

$$I_{ionic} = I_{Cl} + I_{IR} + I_{DR} + I_{Na} + I_{NaK}$$

$$I_{chan} = g_{chan}\,(V - E_{ion}) \qquad \text{chan} \in \{\text{ClC-1, DR, IR, Na}\}$$

$$E_{ion} = \frac{RT}{F}\ln\frac{[ion]_o}{[ion]_i} \qquad ion \in \{Cl^-, K^+, Na^+\}$$

$$g_{Cl} = \hat{g}_{Cl}\,a^4$$

$$g_{IR} = \hat{g}_{IR}\,y$$

$$\hat{g}_{IR} = \frac{G_K\,[K]_R^2}{K_K + [K]_R^2}$$

$$y = 1 - \left[1 + \frac{K_S}{[S]_i^2\,e^{2(1-\delta)VF/RT}}\left(1 + \frac{[K]_R^2}{K_K}\right)\right]^{-1}$$

$$[K]_R = [K]_o\,e^{-\delta E_K\,F/RT}$$

$$[K]_R = [K]_o\,e^{-\delta E_K\,F/RT}$$

$$g_{DR} = \hat{g}_K\,n^4\,h_K$$

$$g_{Na} = \hat{g}_{Na}\,m^3\,h\,S$$

$$I_{NaK} = \hat{I}_{NaK}\,f\,(V)$$

$$\hat{I}_{NaK} = \frac{F\,\hat{J}_{NaK}}{(1 + K_{mK}/[K]_o)^2\,(1 + K_{mNa}/[Na]_i)^3}$$

$$f\,(V) = (1 + 0.12\,e^{-0.1\,VF/RT} + 0.04\,\sigma\,e^{-VF/RT})^{-1}$$

$$\sigma = \frac{1}{7}\,(e^{[Na]_o/67.3} - 1)$$

$$I_T = \frac{V - V_t^{20}}{R_a}$$

$$I_{m,t}^i = \frac{(V_t^{i+1} - 2\,V_t^i + V_t^{i-1})\,g_{L,t}^i}{A_t^i} = I_{C,t}^i + I_{ionic,t}^i$$

$$A_t^i = \frac{\rho\,Vol^i}{\zeta}$$

$$Vol^i = \pi\,\Delta x\,(r_i^2 - r_{i-1}^2)$$

$$g_{L,t}^i = \frac{2\pi\,r_i\,\Delta x\,\overline{G}_L}{r/20}$$

$$\overline{G}_L = \rho\,\sigma_T\,G_L$$

$$I_{C,t}^i = C_m\,\frac{dV_t^i}{dt}$$

$$I_{ionic,t}^i = I_{Cl,t}^i + I_{IR,t}^i + I_{DR,t}^i + I_{Na,t}^i + I_{NaK,t}^i$$

$$\hat{g}_{chan,t} = \eta_{chan}\,\hat{g}_{chan} \qquad \text{chan} \in \{\text{ClC-1, IR, DR, Na}\}$$

$$\frac{d[K^+]_t^i}{dt} = \frac{I_{IR,t}^i + I_{DR,t}^i - 2\,I_{NaK,t}^i}{1000\,F\,\zeta} - \frac{[K^+]_t^i - [K^+]_t^{i+1}}{\tau_K} - \frac{[K^+]_t^i - [K^+]_t^{i-1}}{\tau_K}$$

Table A2-1 Descriptions of the gating processes and parameters

$x \in \{h, m, n\}$	$\frac{dx}{dt} = \alpha_x\,(1 - x) - \beta_x\,x$	
$x \in \{m, n\}$	$\alpha_x = \frac{\hat{\alpha}_x\,(V - V_x)}{1 - e^{\frac{-(V - V_x)}{K\,\alpha_x}}}$	$\beta_x = \hat{\beta}_x\,e^{\frac{-(V - V_x)}{K\,\beta_x}}$
h	$\alpha_h = \hat{\alpha}_h\,e^{\frac{-(V - V_h)}{K\,\alpha_h}}$	$\beta_h = \frac{\hat{\beta}_h}{1 + e^{\frac{-(V - V_h)}{K\,\beta_h}}}$
$x \in \{a, h_\infty, S_\infty\}$ $z \in \{h_K, S\}$	$x = \frac{1}{1 + e^{\frac{V - V_x}{A_x}}}$	$\frac{dz}{dt} = \frac{z_\infty - z}{\tau_z}$
time constants :	$\tau_S = \frac{60}{0.2 + 5.65\left(\frac{V + 90}{100}\right)^2}$	$\tau_{h_K} = e^{\frac{-(V + 40)}{25.75}}$

Appendix 3: Parametrical information

Table A3-1 Gating parameters[a]

Symbol	Unit	$x=a$[b]	$x=h$	$x=h_K$[c]	$x=m$	$x=n$	$x=S$[d]
A_x	mV	150	–	7.5	–	–	5.8
K_{α_x}	mV	–	14.7	–	10	7	–
K_{β_x}	mV	–	9	–	18	40	–
V_x	mV	70	−45	−40	−46	−40	−78
$\hat{\alpha}_x$	$ms^{-1}\,mV^{-1}$	–	–	–	0.288	0.0131	–
$\hat{\alpha}_x$	ms^{-1}	–	0.0081	–	–	–	–
$\hat{\beta}_x$	ms^{-1}	–	4.38	–	1.38	0.067	–

[a] Parameters *h*, *m* and *n* from Cannon et al. (1993)
[b] Pusch et al. (1994) with a shifted *I-V* curve to match E_{Cl}
[c] Adrian et al. (1970)
[d] Found empirically by fitting a Boltzmann distribution function to experimental data (Ruff et al. 1988) with a shifted V_S to match the resting membrane potential

Table A3-2 Conductances and affiliated parameters[a]

Symbol	Unit	Sodium	Potassium		Chloride	Na-K pump
			DR	IR		
E_{ion}	mV	59.3	–81.8		–78.3	–
$\hat{g}$	mS/cm^2	268[b]	21.6[c]	–	6.55[d]	–
G_K	mS/cm^2	–	–	3.7[e]	–	–
$[ion]_o$	mM	133	5.9		128	–
$[ion]_i$	mM	12.7	150.9		5.7	–
$\hat{J}_{NaK}$	$\mu mol/cm^2 s$	–	–	–		207×10^{-6}[d]
K_K	mM^2	–	–	950[e]	–	–
K_{mK}	mM	–	–		–	1[d]
K_{mNa}	mM	–	–		–	13[d]
K_S	mM^2	–	–	1[e]	–	–
$[S]_i$	mM	–	–	10[e]	–	–
δ		–	–	0.4[e]	–	–
η		0.1[c]	0.45[d]	1.0[f]	0.1[g]	0.1[h]
τ_K	ms	–	350[c]		–	–

[a] $[Na^+]_i$, $[K^+]_i$, E_{Na} and E_K from Ward and Wareham (1985), $[Na^+]_o$ and $[K^+]_o$ calculated with the Nernst equation; E_{Cl} is chosen close to the resting membrane potential, as measured by Ward and Wareham (1985): −78.5 mV
[b] Obtained by dividing the value 150 mS/cm^2 (Cannon et al. 1993) by the value of *S* (slow inactivation Na channels) at the resting membrane potential
[c] Cannon et al. (1993)
[d] Results from test simulations
[e] Standen and Stanfield (1978)
[f] Ashcroft et al. (1985)
[g] See description of ClC-1 in text
[h] Fambrough et al. (1987)

Table A3-3 Physical and other parameters

Symbol	Unit	Value
C_m	$\mu F/cm^2$	1[a]
F	C/mol	96485
G_L	mS/cm	3.7[b]
l_f	cm	0.56[b]
r	cm	20×10^{-4}[c]
R	$J\,K^{-1}\,mol^{-1}$	8.31441
R_a	$\Omega\,cm^2$	150[a]
R_i	Ω cm	125[d]
R_e	Ω cm	0[e]
T	K	293
Δx	cm	100×10^{-4}[b]
ζ	cm	10^{-6}[f]
ρ	–	0.003[g]
σ_T	–	0.34[g]

[a] Cannon et al. (1993)
[b] Results from test simulations
[c] Dulhunty (1984)
[d] Conte Camerino et al. (1989)
[e] Model assumption
[f] Peachey (1965)
[g] Mathias et al. (1977)

Acknowledgements The authors thank Truus Steijlen, Willem van Riel and John Baxter for their expert help.

References

Adrian RH, Chandler WK, Hodgkin AL (1970) Voltage clamp experiments in striated muscle fibres. J Physiol (Lond) 208:607–644
Adrian RH, Peachey LD (1973) Reconstruction of the action potential of frog sartorius muscle. J Physiol (Lond) 235:103–131
Adrian RH, Marshall MW (1976) Action potentials reconstructed in normal and myotonic muscle fibers. J Gen Physiol 258:125–143
Ashcroft FM, Heiny JA, Vergara J (1985) Inward rectification in the transverse tubular system of frog skeletal muscle studied with potentiometric dyes. J Physiol (Lond) 359:269–291
Barchi RL (1994) The muscle fiber and disorders of muscle excitability. In: Siegel GJ et al (eds) Basic neurochemistry: molecular, cellular and medical aspects. Raven Press, New York, pp 703–722
Bretag AH (1987) Muscle chloride channels. Physiol Rev 67:618–724
Cannon SC, Brown RH Jr, Corey DP (1993) Theoretical reconstruction of myotonia and paralysis caused by incomplete inactivation of sodium channels. Biophys J 65:270–288
Clausen T (1996) Long- and short-term regulation of the Na^+-K^+ pump in skeletal muscle. News Physiol Sci 11:24–30
Conte Camerino D, De Luca A, Mambrini M, Vrbova G (1989) Membrane ionic conductances in normal and denervated skeletal muscle of the rat during development. Eur J Physiol 413:568–570
Davies NW (1992) ATP-dependent K^+ channels and other K^+ channels of muscle: how exercise may modulate their activity. Med Sport Sci 34:1–10
De Luca CJ, Erim Z (1994) Common drive of motor units in regulation of muscle force. Trends Neurosci 17:299–305
Dulhunty AF (1979) Distribution of potassium and chloride permeability over the surface and T-tubule membranes of mammalian skeletal muscle. J Membr Biol 45:293–310
Dulhunty AF (1984) Heterogeneity of T-tubule geometry in vertebrate skeletal muscle fibres. J Muscle Res Cell Mot 5:333–347
Fahlke C, Rüdel R (1995) Chloride currents across the membrane of mammalian skeletal muscle fibres. J Physiol (Lond) 484:355–368

Fambrough DM, Wolitzky BA, Tamkin MM, Takeyasu K (1987) Regulation of the sodium pump in excitable cells. Kidney Int 32 [suppl. 23]: S97–S112

Fitts RH (1994) Cellular mechanisms of muscle fatigue. Physiol Rev 74: 49–94

Grafe P, Quasthoff S, Grosskreutz J, Alzheimer C (1997) Function of the hyperpolarization-activated inward rectification in nonmyelinated peripheral rat and human axons. J Neurophysiol 77: 421–426

Gurnett CA, Kahl SD, Anderson RD, Campbell KP (1995) Absence of the skeletal muscle sarcolemma chloride channel ClC-1 in myotonic mice. J Biol Chem 270: 9035–9038

Henneberg K, Roberge FA (1997) Simulation of propagation along an isolated skeletal muscle fiber in an isotropic volume conductor. Ann Biomed Eng 25: 15–28

Hicks H, McComas AJ (1988) Increased sodium pump activity following repetitive stimulation of rat soleus muscles. J Physiol (Lond) 414: 337–349

Juel C (1986) Potassium and sodium shifts during in vitro isometric muscle contraction, and the time course of the ion-gradient recovery. Pflügers Arch 406: 458–463

Kirsch GE, Nichols RA, Nakajima S (1977) Delayed rectification in the transverse tubules. J Gen Physiol 70: 1–21

Läuger P (1991) Electrogenic ion pumps. Sinauer Associates, Sunderland, Mass

Luff AR, Atwood HL (1972) Membrane properties and contraction of single muscle fibers in the mouse. Am J Physiol 222: 1435–1440

Luo CH, Rudy Y (1994) A dynamic model of the cardiac ventricular action potential. Circ Res 74: 1071–1096

Mathias RT, Eisenberg RS, Valdiosera G (1977) Electrical properties of frog skeletal muscle fibers interpreted with a mesh model of the tubular system. Biophys J 17: 57–93

Matsuda H, Stanfield PR (1989) Single inwardly rectifying potassium channels in cultured muscle cells from rat and mouse. J Physiol (Lond) 414: 111–124

McKenna MJ (1992) The roles of ionic processes in muscular fatigue during intense exercise. Sports Med 13: 134–145

McKillen HC, Davies NW, Stanfield PR, Standen NB (1994) The effect of intracellular anions on ATP-dependent potassium channels of rat skeletal muscle. J Physiol (Lond) 479: 341–351

Mil HGJ van (1997) The inward potassium rectifier and bistability in the resting membrane potential of skeletal muscle cells. PhD thesis, University of Amsterdam, The Netherlands

Nakajima S, Gilai A (1980) Radial propagation of muscle action potential along the tubular system examined by potential-sensitive dyes. J Gen Physiol 76: 751–762

Nakao M, Gadsby DC (1989) [Na] and [K] dependence of the Na/K pump current-voltage relationship in guinea pig ventricular myocytes. J Gen Physiol 94: 539–565

Peachey LD (1965) The sarcoplasmic reticulum and transverse tubules of the frog's sartorius. J Cell Biol 25: 209–231

Pusch M, Steinmeyer K, Jentsch TJ (1994) Low single channel conductance of the major skeletal muscle chloride channel, ClC-1. Biophys J 66: 149–152

Ruff RL, Simoncini L, Stühmer W (1988) Slow sodium channel inactivation in mammalian muscle: a possible role in regulating excitability. Muscle Nerve 11: 502–510

Seabrooke SR, Ward MR, White NK (1988) The effect of sodium pump blockade and denervation on the steady-state sodium permeability of mouse skeletal muscle fibres. Q J Exp Physiol 73: 561–572

Siegenbeek van Heukelom J (1994) The role of the potassium inward rectifier in defining cell membrane potentials in low potassium media, analyzed by computer simulation. Biophys Chem 50: 345–360

Sjøgaard G, McComas AJ (1995) Role of interstitial potassium. In: Gandevia SC, Enoka RM, McComas AJ, Stuart DE, Tomas CK et al (eds) Fatigue. Neural and muscular mechanisms. Plenum Press, New York, pp 69–80

Standen NB, Stanfield PR (1978) Inward rectification in skeletal muscle: a blocking particle model. Pflügers Arch 378: 173–176

Ward KM, Wareham AC (1985) Changes in membrane potential and potassium and sodium activities during postnatal development of mouse skeletal muscle. Exp Neurol 89: 554–568

Wieland SJ, Gong Q-H (1995) Modulation of a potassium conductance in developing skeletal muscle. Am J Physiol 268 (Cell Physiol 37): C490–C495

Wolters H, Wallinga W, Ypey DL, Boom HBK (1994) Ionic currents during action potentials in mammalian skeletal muscle fibres analysed with loose patch clamp. Am J Physiol 267 (Cell Physiol 36): C1699–C1706

Yasui K, Anno T, Kamiya K, Boyett MR, Kodama I, Toyama J (1993) Contribution of potassium accumulation in narrow extracellular spaces to the genesis of nicorandil-induced large inward tail current in guinea-pig ventricular cells. Pflügers Arch 422: 371–379